Molecular Pharmacology Fast Forward. Published on December 30, 2013 as doi:10.1124/mol.113.090605

MOL # 90605

Triapine and a more potent dimethyl derivative induce ER stress in cancer cells

Robert Trondl, Lea S. Flocke, Christian R. Kowol, Petra Heffeter, Ute Jungwirth, Georg E. Mair, Ralf Steinborn, Éva A. Enyedy, Michael A. Jakupec, Walter Berger and Bernhard K. Keppler

Institute of Inorganic Chemistry, University of Vienna, Währinger Strasse 42, A-1090 Vienna, Austria (RT, LSF, CRK, MAJ, BKK)

Research Platform "Translational Cancer Therapy Research", University of Vienna, Währinger Strasse 42, A-1090 Vienna, Austria and Medical University of Vienna, Borschkegasse 8a, A-1090 Vienna (RT,CRK, PH, UJ, MAJ, WB, BKK)

Institute of Cancer Research, Medical University of Vienna, Borschkegasse 8a, A-1090 Vienna (PH, UJ, WB)

Comprehensive Cancer Centre of the Medical University of Vienna, Vienna, Austria (PH, UJ, WB)

VetCore Facility for Research, VetOmics, University of Veterinary Medicine, Veterinärplatz 1, A-1210 Vienna, Austria (GEM, RS)

Department of Inorganic and Analytical Chemistry, University of Szeged, Dóm tér 7, H-6720 Szeged, Hungary (EAE)

Hungarian Academy of Science-USZ Bioinorganic Chemistry Research Group, Dóm tér 7, H-6720 Szeged, Hungary (EAE)

Running Title: ER stress induction by Triapine and its dimethyl derivative

Address correspondence to author: Michael Jakupec PhD, Institute of Inorganic Chemistry, University of Vienna, Waehringer Strasse 42, Vienna 1090, Austria Tel: +43 1 4277 52610, Fax: +43 1 4277 52680; E-mail: michael.jakupec@univie.ac.at

Number of text pages: 26

Number of tables: 0

Number of figures: 5

Number of references: 48

Word count (Abstract): 248

Word count (Introduction): 749

Word count (Discussion): 1224

Abbreviations: 3-AP, Triapine; 3-AP-Me, N^4,N^4-dimethyl-Triapine; ATF4, activating transcription factor 4; ATF6, activating transcription factor 6; BIM, bcl-2 interacting mediator of cell death; CHOP, CCAAT/enhancer-binding protein homologous protein; DCF-DA, 2´,7´-dichlorofluorescein diacetate; ER, endoplasmic reticulum; GRP78, ER-resident chaperon glucose-regulated protein 78 kDa; JC-1, 5,5,6,6-tetrachloro-1,1,3,3-tetraethylbenzimidazol-carbocyanine iodide; JNK, JUN N-terminal kinase; NAC, N-acetyl cysteine; eIF2α, eukaryotic translation initiation factor 2 alpha; PERK, PRKR-like endoplasmic reticulum kinase; RT-qPCR, reverse transcription quantitative real-time PCR; ROS, reactive oxygen species; UPR, unfolded protein response; XBP1, X-box binding protein 1

Abstract

Triapine (3-AP), a ribonucleotide reductase inhibitor, has been extensively evaluated in clinical trials in the last decade. This study addresses the role of ER stress in the anticancer activity of 3-AP and the derivative 3-AP-Me, differing from 3-AP only by dimethylation of the terminal nitrogen. Treatment of colon cancer cells with 3-AP or 3-AP-Me activated all three ER stress pathways (PERK, IRE1a and ATF6) by phosphorylation of eIF2α and upregulation of ATF4 and ATF6 gene expression, and particularly 3-AP-Me lead to an upregulation of the alternatively spliced mRNA variant XBP1s (16-fold). Moreover, 3-AP and 3-AP-Me activated the cellular stress kinases JNK and p38 MAPK, and inhibition of JNK activity antagonized the cytotoxic effect of both compounds. Subsequent to induction of the unfolded protein response (UPR), a significant upregulation of pro-apoptotic proteins was detected, including the transcription factor CHOP and the BH3-only member protein Bim, an essential factor for ER stress-related apoptosis. In correlation with the higher degree of ER stress after 3-AP-Me treatment, also a more potent depolarization of mitochondrial membranes was found. These data suggest that 3-AP and 3-AP-Me induce apoptosis via ER stress. This was further corroborated by showing that inhibition of protein biosynthesis with cycloheximide prior to 3-AP and 3-AP-Me treatment leads to a significant reduction of the anti-proliferative properties of both compounds. Taken together, this study demonstrates that induction of ER stress contributes to the mode of action of 3-AP and that terminal methylation leads to an even more pronounced manifestation of this effect.

Introduction

Triapine (3-AP; Fig. 1A) belongs to the large class of α-N-heterocyclic thiosemicarbazones. Its antitumor activity has been known for more than a decade and was studied in several clinical phase I and phase II trials (Nutting *et al.*, 2009; Kunos *et al.*, 2010; Traynor *et al.*, 2010; Ocean *et al.*, 2011). The anticancer activity of 3-AP has been attributed to the inhibition of the ribonucleotide reductase enzyme (Finch *et al.*, 2000). Human ribonucleotide reductase is a tetramer consisting of two large subunits (hRRM1) bearing the substrate binding site and two small subunits (hRRM2 or p53R2) containing the catalytically active site which harbors a tyrosyl radical stabilized by a di-iron center (Eklund *et al.*, 2001). This enzyme catalyzes the reduction of ribonucleotides to deoxyribonucleotides, which are required for DNA synthesis. Due to a higher demand for DNA replication and repair in tumor cells, ribonucleotide reductase is a suitable and well-established molecular target for cancer therapy. It can be inhibited by radical scavengers which interfere with the tyrosyl radical (e.g. hydroxyurea), nucleoside and nucleotide analogues (e.g. gemcitabine, cytarabine), and iron chelators (e.g. desferrioxamine) which interact with the iron center of the enzyme (Wijerathna *et al.*, 2011). For α-N-heterocyclic thiosemicarbazones such as 3-AP, the suggested mode of action is the intracellular formation of very stable iron complexes and subsequent generation of reactive oxygen species (ROS) which inhibit ribonucleotide reductase by destruction of the tyrosyl radical (Shao *et al.*, 2006). Electron paramagnetic resonance (EPR) spectroscopy measurements of 3-AP-treated neuroepithelioma cells have demonstrated a decrease of the tyrosyl radical to 61% of the control, comparable to the effect of the pyridoxal isonicotinoyl class iron chelator 311; but whereas the addition of iron decreased the cytotoxicity of the iron chelators desferrioxamine and 311, iron supplementation prior to 3-AP treatment had no significant effects on its cytotoxicity (Chaston *et al.*, 2003). Furthermore, hydroxyurea-resistant cell lines overexpressing the hRRM2 subunit of ribonucleotide reductase showed no resistance to 3-AP (Yen *et al.*, 1994; Finch *et al.*, 1999), and analysis of recombinant ribonucleotide reductase by EPR spectroscopy revealed that 3-AP does not significantly remove iron from

hRRM2 (Shao *et al.*, 2006). The complexity of these findings indicates that, in addition to ribonucleotide reductase inhibition, further mechanisms may contribute to the activity of 3-AP.

In previous studies, we demonstrated that chemical modification of various thiosemicarbazones by dimethylation of the terminal amino group has a strong impact on their biological activity (Kowol *et al.*, 2009). In the present study, we show that 3-AP and its dimethylated derivative 3-AP-Me particularly co-localize with mitochondria and endoplasmic reticulum (ER), which inspired us to further examine the impact of the two drugs on the ER.

One of the functions of the ER is folding of secreted and resident proteins into their native structures and the corresponding quality control of newly synthesized proteins (Ellgaard and Helenius, 2003). ER stress is induced by the accumulation of misfolded and/or unfolded proteins in the ER lumen, which leads to disruption of ER homeostasis. Subsequently, the unfolded protein response (UPR) is initiated by dissociation of the ER-resident chaperone glucose-regulated protein 78 kDa (GRP78) from the three ER transmembrane proteins PERK, IRE1a, and ATF6 (Szegezdi *et al.*, 2006; Ron and Walter, 2007). This cellular response is followed by the upregulation of ER-related chaperones and inhibition of the translation machinery to restore correct protein folding and ER homeostasis. However, severe ER stress (e.g. initiated by cytotoxic agents) leads to a change in the UPR pathway from pro-survival to pro-apoptotic signaling (Xu *et al.*, 2005). In this context, the transcription factor CHOP (CCAAT/enhancer-binding protein homologous protein, also called GADD153) is crucial for switching to pro-apoptotic signaling (Oyadomari and Mori, 2004). CHOP is strongly associated with induction of ER stress-mediated apoptosis by altering the balance between pro-survival and pro-apoptotic bcl-2 family members and by stimulating death receptor 5 (DR5) (McCullough *et al.*, 2001; Yamaguchi and Wang, 2004; Puthalakath *et al.*, 2007). Due to high metabolic activity and elevated levels of chronic stress in cancer cells, targeting the ER stress response is a new promising strategy against cancer (Healy *et al.*, 2009).

In this study, we demonstrate that treatment of cancer cells with 3-AP (Fig. 1) leads to a pronounced expression of proteins associated with ER stress and ER stress-mediated apoptosis and to depolarization of mitochondrial membranes. These effects can be observed to an even stronger extent when the

dimethylated derivative 3-AP-Me is applied instead of 3-AP. These findings suggest a hitherto overlooked role of ER stress as a novel molecular mechanism of α-N-heterocyclic thiosemicarbazones.

Materials and methods

Reagents and antibodies. 3-AP and 3-AP-Me were synthesized as reported previously (Kowol *et al.*, 2009). Both compounds were dissolved in DMSO and then diluted in cell culture medium to obtain the indicated concentrations. All cell culture media and solutions were purchased from Sigma-Aldrich Austria. Calnexin, Calreticulin, PERK, p-eIF2α, total eIF2-α, p-p38 MAPK, total p38 MAPK, GRP78, p-JNK, total JNK, Bim and β-actin antibodies were purchased from Cell Signaling Technology (Danvers, MA). CHOP antibody, cycloheximide (CHX) and JNK inhibitor SP600125 were purchased from Abcam (Cambridge, UK). Horseradish peroxidase-labeled anti-mouse IgG and anti-rabbit IgG secondary antibodies were purchased from Cell Signaling Technology. Thapsigargin was obtained from Sigma Aldrich (Vienna, Austria).

Cell culture conditions. SW480, HCT-116 (both colon carcinoma, human) and HL-60 cells (promyelocytic leukemia, human) were purchased from the American Type Culture Collection (ATCC). Cells were grown in Eagle's Minimal Essential Medium (MEM) supplemented with 10% heat-inactivated fetal bovine serum, 1 mM sodium pyruvate, 4 mM L-glutamine, and 1% nonessential amino acids (from 100x ready-to-use stock solution) in a humidified incubator at 37°C and 5% CO_2. For cell culture experiments, exponentially grown cells were washed with phosphate buffered saline (PBS) before used in the methods described below.

Fluorescence microscopy. SW480 cells were cultured on cover slips in 6-well plates (Starlab, Hamburg, Germany). A flow cell slide was used for stepwise staining of the cell population. Fluorescence microscope BX40 with F-View CCD Camera, Cell^F fluorescence imaging software and 60x magnification oil immersion objective lens (all from Olympus, Vienna, Austria) were used. Cells were

incubated with 100 µM 3-AP and 3-AP-Me in MEM for 5 min and washed three times with PBS before image acquisition. ER-Tracker Green and Mito-Tracker Red (Invitrogen, Vienna, Austria) were used according to the instructions of the manufacturer. Use of a flow cell microscope slide allowed a stepwise staining procedure and prevented bleed-through of fluorochromes.

Measurement of intracellular oxidants. 2´,7´-Dichlorofluorescein diacetate (DCF-DA) was used to detect the production of ROS (Gomes *et al.*, 2005). DCF-DA stock solutions (33.4 mM, DMSO) were stored at –20 °C. HL60 cells (2.5×10^5 cells per sample in phenol-free Hanks balanced salt solution) were incubated with DCF-DA (1 µM) for 30 min. Subsequently, the compounds were added in the indicated concentrations. After incubation for another 30 min, mean fluorescence intensity was measured by flow cytometry using a fluorescence-activated cell sorting (FACS) Calibur instrument (Becton Dickinson, Schwechat, Austria). A concentration of 200 µM H_2O_2 was used as positive control. The resulting histograms were quantified by using the ModeFit software (BD).

Western blot analysis. 2.5×10^5 SW480 cells were seeded 24 h prior to treatment into 6-well plates. Cells were exposed to 1, 5, 25 and 50 µM 3-AP or 3-AP-Me for different incubation times. Thapsigargin (0.5 µM) was used as a positive control. Total cell lysates were prepared by lysis with radioimmunoprecipitation assay (RIPA) buffer including protease and phosphatase inhibitor cocktails (Sigma-Aldrich). Identical amounts of total proteins were resolved by SDS-PAGE and electrophoretically transferred onto a nitrocellulose membrane by using a semi-dry blotter (Peqlab, Erlangen, Germany). The membrane was blocked with 5% BSA in TBST buffer for 1 h at room temperature. Primary antibodies were diluted according to the instructions of the manufacturer and incubated overnight at 4 °C. Anti-β-actin was used as a loading control. Secondary antibodies were appropriately diluted and incubated for 1 h at room temperature. Horseradish peroxidase-coupled secondary antibodies were detected by chemiluminescence using Super Signal chemiluminescence substrate from Pierce and chemiluminescence detection system Fusion SL (Vilber Lourmat, Eberhardzell, Germany).

Cytotoxicity tests in cancer cell lines. Cytotoxic effects of the test compounds together with protein synthesis and JNK inhibitors were determined by means of a colorimetric microculture assay [MTT assay, MTT = 3-(4,5-dimethyl-2-thiazolyl)-2,5-diphenyl-2H-tetrazolium bromide]. Cells grown as adherent monolayer in 75 cm^2 flasks (Starlabs, Hamburg, Germany) were harvested by trypsinisation. By using a pipetting system (Biotek Precision XS Microplate Sample Processor), and densities of 2×10^3 cells (HCT-116) were seeded in triplicate 100 µl aliquots into 96-well microculture plates (Starlabs, Hamburg, Germany). Before drug exposure, cells were allowed to settle and attach to plates in drug-free complete culture medium for 24 h. Test compounds were dissolved in distilled water prior to the preparation of a serial dilution in complete culture medium. The dilution series as well as the pipetting steps were done by the microplate processor. After 96 h of exposure, the medium was removed and replaced by 100 µl 1:7 MTT/RPMI-1640 solution (MTT solution: 5 mg/ml MTT in phosphate buffered saline) for 4 h incubation at 37 °C in a humidified atmosphere containing 5% CO_2. Subsequently, the MTT/RPMI solution was removed from all wells and the formazan crystals formed by viable cells were dissolved in 150 µl DMSO per well. Optical densities at 550 nm were measured with a microplate reader (Biotek ELx808), by using a reference wavelength of 690 nm to correct for unspecific absorption. The quantity of viable cells was expressed in terms of the T/C values by a comparison to untreated control microcultures, and 50% inhibitory concentrations (IC_{50}) were calculated from concentration-effect curves by interpolation. Evaluation is based on means from at least three independent experiments.

RT-qPCR. Sequences of primers and hydrolysis probes (Supplemental Tables 1;2) were designed with Primer Express version 2.0 software (Applied Biosystems, Vienna, Austria). Primers were analyzed for all primer secondary structures including hairpins, self-dimers, and cross-dimers in primer pairs using NetPrimer software (Premier Biosoft, Palo Alto, CA) and for specificity using Primer-BLAST of NCBI. Amplicon secondary structure was assessed with mfold web server (Zuker, 2003).

Treated and mock-treated SW480 cells were lyzed with QIAzol (Qiagen, Vienna, Austria). For automated isolation of total RNA the miRNeasy Kit (Qiagen, Vienna, Austria) was used on the QIAcube robot

(Qiagen, Vienna, Austria). RNA amount was measured spectrophotometrically with the BioPhotometer 6131 combined with the TrayCell cuvette (Eppendorf, Vienna, Austria; Hellma Worldwide, Müllheim, Germany). RNA integrity number (RIN) determined with the RNA 6000 Nano Chip Kit (Agilent Technologies) on the 2100 Bioanalyzer (Agilent Technologies, Vienna, Austria) was ≥ 7 for experimental samples. The High-Capacity Reverse Transcription Kit (Applied Biosystems, Vienna, Austria) was used for random hexamer primed cDNA synthesis incubated at 37 °C for 120 min. The 20 µl multiplexed qPCR consisted of Rotor Gene Multiplex PCR Kit (Qiagen, Vienna, Austria), 150 nM of each primer, 150 nM target probe, 150 nM reference gene probe and was performed with 10 ng cDNA triplicates. For qPCR conducted on the ViiA7 Real-Time PCR System (Applied Biosystems, Vienna, Austria), a temperature protocol with an initial hot start at 95 °C for 5 min followed by 50 amplification cycles (95°C for 15 s, 58 °C for 25 s, 60 °C for 25 s) was used. High resolution melting curve analysis was performed to ensure specificity. Target expression was normalized by the reference gene TATA box binding protein, TBP (Kwon *et al.*, 2009) which displayed minimal variation across experimental groups ($\Delta Cq < 0{,}84$). A series of five eight-fold dilutions of a control cDNA from mock-treated SW480 or HCT-116 cells amplified in triplicate was used to generate a standard curve. Reaction efficiencies (E) calculated from the slope of the standard curve using the formula $E = 10^{-1/slope}$ ranged from 84% to 100% (Supplemental Table 2). Calculation of expression changes and evaluation of their statistical significance were performed using the Relative Expression Software Tool (REST) 2007 software including the Pair Wise Fixed Reallocation Randomisation Test (Pfaffl *et al.*, 2002). Finally, the *n*-fold expression change of the two splicing variants was given relative to the untreated control group.

Analysis of mitochondrial membrane potential. Depolarization of mitochondrial membrane potential was determined by FACS analysis using JC-1 (5,5,6,6-tetrachloro-1,1,3,3-tetraethylbenzimidazol-carbocyanine iodide, Biovision), which forms in intact mitochondria multimer J-aggregates emitting fluorescent light at 590 nm. Loss of mitochondrial membrane potential leads to dissociation of J-aggregates to monomers, which implicates a change in the emission wavelength to 527 nm (Salvioli *et al.*,

1997). For this purpose, HL-60 cells were treated with 0.25, 0.5, and 1 µM 3-AP or 3-AP-Me for 24 h. After treatment, cells were pelleted, washed with PBS and stained with 2 µg/ml JC-1 for 20 min at 37 °C. After staining, cells were washed twice with PBS and analyzed with a Guava 8HT flow cytometer (Millipore, Vienna, Austria). Results were repeated in three independent experiments, and statistical analysis was performed with FlowJo software.

Statistical analysis. Error bars represent the standard error of the arithmetic mean (SEM). One-way ANOVA were used for statistical analysis using GraphPad Prism Version 5.0 (GraphPad Software).Values of P less than 0.05 were considered to represent statistically significant differences.

Results

Co-localization of 3-AP and 3-AP-Me with ER and mitochondria. We found that 3-AP-Me has similar intrinsic fluorescence properties in terms of maximum excitation and emission wavelengths as the already reported 3-AP (Fig. 1) (Kowol *et al.*, 2010). Intracellular distribution of both compounds was examined in SW480 colon carcinoma cells by fluorescence microscopy in a live cell setting (Fig. 2). The cellular uptake of both compounds was remarkably quick (within 5 min), and longer incubation times did not improve the image quality. Sequential co-staining in a flow chamber with ER-Tracker Green and Mito-Tracker Red was used to study the co-localization with organelles of both compounds and prevented interference of the fluorochromes. Microscopic images (Fig. 2) show a preferred localization of both compounds in structures of the cytoplasm. While 3-AP accumulated in more granular structures, which match with mitochondria (see zoomed details in Fig. 2A); on the contrary, images of 3-AP-Me show a mesh-like structure comparable with the structures observed with ER-Tracker Green. Thus, intracellular distribution on the light microscopy scale suggests a direct interaction of both compounds with ER and/or mitochondria.

3-AP and 3-AP-Me induce pro-apoptotic signaling of the unfolded protein response. The comparable cytotoxicity of 3-AP and 3-AP-Me is an optimal basis for studying differences in their molecular mechanisms of action. Protein levels and mRNA expression of key factors of the UPR were determined to assess the influence of 3-AP and 3-AP-Me on ER homeostasis (Fig. 3). As activation of UPR proteins is strongly time-dependent, different time points for Western blot analysis were chosen. The ER stress inducer thapsigargin was used as a positive control. As shown in Figure 3, a concentration of 1 µM of 3-AP-Me led to an activation of PERK in HCT-116 cells, whereas only a slight activation of PERK was observed in SW480. 3-AP-Me treatment resulted in both cell lines in phosphorylation of eIF-2α, a downstream target of PERK and suppressor of the protein translation machinery. In contrast, 3-AP only slightly increased eIF-2α phosphorylation at the highest tested concentration (25 µM). Enhanced expression of the lectin ER-chaperon Calreticulin after 3-AP-Me treatment was observed in a similar

pattern as the activation of e-IF2α. 3-AP-Me induced Calnexin upregulation only in HCT-116 cells. Interestingly, after 24 h no or only slight upregulation of the key ER chaperon GRP78 was observed for both compounds, whereas thapsigargin treatment showed a clear induction of this upstream initiator of UPR signaling (Supplemental Figure 1). Higher expression of GRP78 was first detectable after 48 h 3-AP or 3-AP-Me treatment in SW480 cells, with 3-AP-Me again being more active than 3-AP. However, no GRP78 upregulation was observed in HCT-116 cells. In both cell lines, a distinct upregulation of the pro-apoptotic factor CHOP was determined after 24 h 3-AP-Me treatment, while CHOP upregulation in 3-AP-treated cells was only observed at the highest concentration (25 µM).

To address the effects of 3-AP and 3-AP-Me on the transcriptional level of UPR, expression levels of several key factors were quantified by RT-qPCR. Analysis of mRNA expression levels of CHOP and GRP78 confirmed the pro-apoptotic signaling of UPR. After 24 h treatment with 3-AP-Me CHOP mRNA level was found significantly higher in both cell lines (Fig. 3B). 3-AP-Me led to an up to 11-fold upregulation in SW480 cells, whereas 3-AP treatment led only to slightly elevated levels (2-fold). In HCT-116 cells, the highest CHOP expression was found with 25 µM 3-AP treatment. Nevertheless, CHOP overexpression was more pronounced at lower concentrations of 3-AP-Me. However, no significant upregulation of the pro-survival factor GRP78 was observed for both compounds, which is good accordance with the previous observations on the protein level. Together these results provide strong evidence that both compounds induce severe ER stress, and terminal dimethylation (3-AP-Me) strongly increases these effects compared to 3-AP.

3-AP-Me activates transcriptional upregulation program of XBP1, ATF4 and ATF6. The transcription factors ATF4, ATF6, and X-box binding protein 1 (XBP-1) are downstream effectors of UPR signaling and play an essential role in CHOP induction (Oyadomari and Mori, 2004). Substantial ER stress promotes alternative splicing to the 26 bp shorter mRNA variant (141 bp), which results in a frameshift and encodes the bZip transcription factor XBP1s (Yoshida *et al.*, 2001). Fluorescence-labeled probes were designed to quantify the mRNA of the full length XBP1u and the alternatively spliced

XBP1s via RT-qPCR in a duplex reaction. As shown in Figure 3C, 24 h treatment with 3-AP-Me resulted in an up to 16- and 14-fold upregulation of XBP1s in SW480 and HCT-116 cells, respectively. At the same time, a significant downregulation (~10-fold) of XBP1u in both cell lines was observed for 3-AP-Me treatment. On the contrary, 3-AP-treated cells did not upregulate the alternatively spliced XBP1s at any used concentration. Rather, a slight downregulation of XBP1s mRNA was detected after 3-AP treatment. After 8 h no changes in XBP1 splicing was observed (Supplemental Figure 2). Moreover, the transmembrane receptor IRE1a mRNA was found overexpressed (up to 29-fold), and again 3-AP-Me induces a significantly enhanced expression at lower concentrations (Supplemental Figure 3). In good accordance with these findings, analysis of the transcription factors ATF4 and ATF6 displayed a significant upregulation of mRNA expression after 3-AP-Me treatment in SW480 cells. Surprisingly, in HCT-116 cells expression levels for ATF4 and ATF6 were only slightly elevated after 3-AP-Me treatment, whereas high concentrations of 3-AP (25 μM) lead to a significant upregulation of both transcription factors. Taken together, our findings show a distinct induction of UPR transcription factors XBP1, ATF4, and ATF6 for 3-AP-Me treated cells. Activation of the transcriptional upregulation program of IRE1a, ATF4, and ATF6 and the alternative XBP1 splicing demonstrate severe ER stress and a distinct activation of signaling branches of transmembrane receptors IRE1a and ATF-6.

3-AP and 3-AP-Me induce ER stress in a ROS-independent way. ROS can play a critical role in ER stress induction, and generation of ROS via Fenton-like reactions was demonstrated for an iron-3-AP complex previously (Shao *et al.*, 2006). To investigate the role of ROS in the anticancer activity of 3-AP and 3-AP-Me in SW480 cells, the radical scavenger N-acetyl cysteine (NAC) was used. Supplemental Figure 4A shows the H_2O_2 and hydroxyl radical generation after 30 min drug treatment, visualized by the ROS-sensitive dye DCF-DA (Gomes *et al.*, 2005). For neither of the two drugs, a significant increase of intracellular ROS levels could be observed and, thus, NAC co-treatment had no effect in these experiments. Also in 72 h viability assays, co-treatment with NAC did not protect cells from 3-AP or 3-

AP-Me cytotoxicity (Supplemental Figure 4B). Thus, in contrast to the literature, where intracellular ROS generation by the iron-3-AP complex is suggested, our data indicate no significant increase in ROS levels.

3-AP and 3-AP-Me activate the p38 MAPK and JNK pathway and trigger Bim expression. Next, the effects of 3-AP and 3-AP-Me treatment on p38 MAPK and JNK activation were studied. It has been reported that the activation of JNK and p38 MAPK is associated with ER stress and ER stress-initiated cell death (Urano *et al.*, 2000; Maytin *et al.*, 2001; Luo and Lee, 2002). Western blot experiments showed phosphorylation of JNK and p38 MAPK after 12 h incubation with 3-AP or 3-AP-Me (Fig. 4A). Concentration dependency was only observed in the case of 3-AP because 3-AP-Me exerted a much stronger, near maximum effect already at the lowest concentration applied. A sharp decrease in phosphorylated levels of JNK and p38 MAPK at the highest tested concentration of 3-AP-Me (25 µM) in SW480 cells may indicate an already completed stress response. Furthermore, expression of the Bcl-2 protein family member Bim was analyzed, as it is known to be triggered by severe ER stress. Distinct upregulation in a concentration-dependent manner was observed for 3-AP and 3-AP-Me in both cell lines (Fig. 4A). These results indicate a severe cellular stress response and induction of the proapoptotic BH3-only member Bim, which is essential for ER-stress mediated apoptosis (Puthalakath *et al.*, 2007).

Reduced protein burden and inhibition of stress response diminish antiproliferative effects of 3-AP and 3-AP-Me. Subsequently, we investigated if reduced protein biosynthesis and inhibition of cellular stress response have an influence on the antiproliferative effect of 3-AP and 3-AP-Me. For this purpose, cycloheximide (CHX), a protein synthesis inhibitor which thereby reduces the protein load to the ER, and a ATP-competitive JNK inhibitor were used. Co-treatment with each inhibitor reduced the antiproliferative effect of both compounds significantly. The cytotoxicity of 3-AP decreased markedly to IC_{50} values of 15.8 µM (21-fold) or 6.5 µM (8.6-fold) with co-incubation of 10 µM JNK inhibitor or 1.25 µM protein synthesis inhibitor CHX, respectively (Figure 4B). Although the reduction of antiproliferative properties of 3-AP-Me were less pronounced, the increase of IC_{50} values with JNK inhibitor and/or CHX was statistically significant ($p < 0.001$). The combination of the JNK inhibitor and

CHX together inhibited the activity of the thiosemicarbazones not more than each inhibitor alone. These results provide strong evidence that reduced protein load and/or inhibition of cellular stress kinases have a direct impact on the cytotoxic effects of 3-AP and 3-AP-Me.

Dimethylation of 3-AP leads to enhanced depolarization of mitochondrial membranes. Changes in mitochondrial membrane potential ($\Delta\Psi_m$) are key events in apoptosis induction, and recent studies showed that non-resolved ER stress leads to mitochondrial membrane permeabilization and loss of $\Delta\Psi_m$ (Gupta, Cuffe, *et al.*, 2010). To monitor $\Delta\Psi_m$, flow cytometric analysis with the fluorescence dye JC-1 was used in human HL-60 leukemia cells after 24 h treatment with different concentrations (0.25-0.1 µM) of 3-AP or 3-AP-Me. As shown in the contour plots in Figure 5, HL-60 cells treated with 3-AP-Me showed a markedly enhanced depolarization of mitochondrial membranes compared to 3-AP. HL-60 cells displayed a loss of mitochondrial membrane potential of about 30% at a concentration of 0.25 µM of 3-AP-Me. Concentrations of 0.5 and 1 µM resulted in up to 50% of cells with depolarized mitochondrial membranes. In contrast, 0.25 and 0.5 µM of 3-AP caused only a slight or no decrease in $\Delta\Psi_m$. However, 3-AP treatment at 1 µM led to 40% cells with depolarized mitochondrial membranes.

Discussion

In this study, we revealed the subcellular co-localization of 3-AP and its terminal dimethylated derivative 3-AP-Me, with organelle-specific fluorescent trackers, which indicated accumulation of the compounds in the ER and/or mitochondria. To investigate if the cellular site of accumulation is associated with the intracellular site of action, the influence of 3-AP and 3-AP-Me on ER functions, in particular the UPR, was studied for the first time. The UPR can be triggered by a wide variety of causes, including accumulation of misfolded/unfolded proteins, imbalances in ER lipids and glycolipids, changes in the redox environment of ER caused by ROS, and disruption of Ca^{2+} homeostasis. Recent studies showed that Cu^{2+} thiosemicarbazone complexes generate oxidative stress in cell-based assays, whereas the metal-free compounds do not (Hancock *et al.*, 2011; Lovejoy *et al.*, 2011; Kowol *et al.*, 2012). Furthermore, the Cu^{2+}

complex of the thiosemicarbazone NSC 689534 was shown to induce ER stress in a ROS-dependent manner, whereas the metal-free NSC 689534 does neither induce oxidative nor ER stress (Hancock *et al.*, 2011). In contrast, our study revealed that the metal-free thiosemicarbazones 3-AP and 3-AP-Me induce ER stress in a ROS-independent manner. Furthermore, their cytotoxicity was not associated with oxidative stress.

Activation of the UPR was proven by upregulation of several proteins including p-eIF2α, PERK, calreticulin and CHOP. The translation initiation factor eIF2α gets phosphorylated on Ser51 by PERK, a type I transmembrane protein and initiator of UPR (Schmitt *et al.*, 2010). By phosphorylation of the α-subunit of eIF2α the translation of most mRNAs is downregulated to reduce the burden on the stressed ER by decreasing the amount of newly synthesized polypeptides (Boyce and Yuan, 2006). On the other hand, p-eIF2α upregulates ATF4, which in turn stimulates the expression of ER chaperons such as GRP78 to restore ER homeostasis (Harding *et al.*, 2003). However, if the protein machinery is severely disturbed, the pro-survival signaling can switch to a pro-apoptotic pathway by upregulation of CHOP, whose induction strongly depends on ATF4 (Szegezdi *et al.*, 2006). CHOP plays an essential role in ER stress-mediated apoptosis by regulating genes involved in cell life and death decisions (Matsumoto *et al.*, 1996). Western blot analysis displayed a strong upregulation of eIF2α phosphorylation after 3-AP-Me treatment, whereas for 3-AP only a slight increase was observed. Remarkably, upregulated CHOP levels were observed upon 3-AP or 3-AP-Me treatment, whereas no increased expression of GRP78 was observed. In order to overcome acute ER stress, chaperons such as GRP78 are upregulated by the UPR to increase ER folding capacity, and thus high levels of GRP78 are associated with pro-survival signaling of ER stress responses (Lee, 2007; Pyrko *et al.*, 2007). We found increased protein expression of GRP78 only after 48 h treatment in SW480 cells, but not in HCT-116 cells. These results were confirmed by mRNA expression analysis, which showed significantly upregulated levels of the pro-apoptotic factor CHOP and only little or no elevated mRNA levels of GRP78. Increased levels of CHOP without upregulation of GRP78 suggest a severely disturbed ER homoeostasis and indicate an imbalance of anti- and pro-

apoptotic signals in favor of the latter (Suzuki *et al.*, 2007). In contrast to 3-AP and 3-AP-Me, treatment with the ER stress inducer thapsigargin led to upregulation of GRP78 in all used cell lines. Furthermore, reducing the protein load by inhibiting protein synthesis led to a significant reduction of the antiproliferative properties of both compounds. Remarkably, the reduction of cytotoxicity by CHX co-incubation was less pronounced for 3-AP-Me, which is a stronger inducer of ER stress. The distinctly higher induction of ER stress by 3-AP-Me compared to 3-AP supports the assumption that the dimethylamine moiety plays a crucial role in the induction of pro-apoptotic signaling of the UPR.

During ER stress XBP1s regulates several UPR-related genes, such as $p58^{IPK}$, CHOP, and XBP1 itself (Lee *et al.*, 2003). Analysis of both XBP1 mRNA splicing variants by RT-qPCR showed a strong induction of the alternatively spliced variant XBP1s by 3-AP-Me treatment, while in the case of 3-AP no upregulation of XBP1s mRNA was observed. This emphasizes that the dimethylamine moiety is a crucial factor for induction of the IRE1a-XBP1 branch of the UPR. Furthermore, the IRE1a-TRAF2-ASK1 pathway is thought to be coupled with cellular stress-activated protein kinases such as JNK and p38 MAPK, which are assumed to play an important role in ER stress-mediated apoptosis (Urano *et al.*, 2000; Luo and Lee, 2002; Gupta, Deepti, *et al.*, 2010). In accordance with the increased UPR protein expression, both compounds led to elevated levels of phosphorylated p38 MAPK and JNK. After exposure to 3-AP or 3-AP-Me, the activation of JNK and p38 MAPK signaling indicates severe cellular stress. Co-incubation with a JNK inhibitor led to a significant reduction of antiproliferative properties of both compounds.

The close interplay of ER and mitochondria supports signaling between those two organelles for various cellular functions including regulation of ER chaperones, ATP synthesis, and ER stress-induced apoptosis (Gupta, Cuffe, *et al.*, 2010). Recent studies showed that ER stress triggers a loss of mitochondrial membrane potential via multiple signals such as induction of BH3-only proteins (Gupta, Cuffe, *et al.*, 2010). Furthermore, is has been shown that elevated levels of CHOP result in upregulation of pro-apoptotic bcl-2 family member Bim. (McCullough *et al.*, 2001; Gotoh *et al.*, 2004; Puthalakath *et al.*, 2007). In this study, we were able to demonstrate that treatment with 3-AP and 3-AP-Me leads to

upregulation of the pro-apoptotic protein Bim. These findings are in good agreement with increased levels of phosphorylated JNK, which is known for its regulatory functions on members of the bcl-2 protein family (Weston and Davis, 2007). Depolarization of mitochondrial membranes support the concept of ER stress-mediated apoptosis via induction of BH3-only proteins. In good accordance with this concept, it was shown that the enhanced ER stress induction by 3-AP-Me is associated with a more pronounced depolarization of mitochondrial membranes.

In good accordance with our results, mRNA expression studies with the thiosemicarbazone Dp44mT (di-2-pyridylketone-4,4,-dimethyl-3-thiosemicarbazone) suggested that iron depletion is responsible for elevated levels of DITT3 (a synonym for the gene encoding CHOP) (Yu and Richardson, 2011). Indeed, investigations regarding the stability of metal complexes of 3-AP and 3-AP-Me with iron, zinc, and copper revealed that terminally dimethylated thiosemicarbazones such as 3-AP-Me form metal complexes with higher stability (Enyedy *et al.*, 2010, 2011). Both compounds form iron complexes with fairly high stability. Stability of the complexes $[Fe^{II/III}(L)_2]$ (L = 3-AP or 3-AP-Me) can be compared by the overall stability constants ($\log\beta([Fe^{II/III}(L)_2]) - 2\times\log\beta(H_2L)$, which are -6.85 and -5.04 for the Fe^{II} complexes and -2.80 and -0.33 for the Fe^{III} species in the case of 3-AP and 3-AP-Me, respectively. The higher values represent the greater stabilities. The several orders of magnitude higher constants clearly reveal that dimethylation of the terminal nitrogen leads to more stable iron complexes (Enyedy *et al.*, 2011). Metal complexation characteristics of thiosemicarbazones might interfere with proper folding of metalloproteins, and the ability of 3-AP-Me to form metal complexes with higher stability may be responsible for the enhanced ER stress.

Taken together, the severe disruption of the protein folding machinery may represent a new molecular target in addition to the ribonucleotide reductase inhibition potential of thiosemicarbazones. Our results indicate that ER stress and the induction of cellular stress kinases are an additional mechanism of the antitumor activity of the clinically investigated 3-AP, and can be distinctly increased by terminal dimethylation of the compound.

Participated in research design: Trondl, Flocke, Heffeter, Kowol, Jakupec

Conducted experiments: Trondl, Flocke, Heffeter, Jungwirth, Enyedy

Contributed new reagents or analytic tools: Trondl, Flocke, Kowol, Jungwirth, Mair, Steinborn

Performed data analysis: Trondl, Flocke, Heffeter, Mair, Steinborn

Wrote or contributed to the writing of the manuscript: Trondl, Flocke, Kowol, Heffeter, Jungwirth, Mair, Steinborn, Enyedy, Jakupec, Berger, and Keppler.

References

Boyce M, and Yuan J (2006) Cellular response to endoplasmic reticulum stress: a matter of life or death. *Cell Death Differ* **13**:363–373.

Chaston TB, Lovejoy DB, Watts RN, and Richardson DR (2003) Examination of the Antiproliferative Activity of Iron Chelators: Multiple Cellular Targets and the Different Mechanism of Action of Triapine Compared with Desferrioxamine and the Potent Pyridoxal Isonicotinoyl Hydrazone Analogue 311. *Clin Cancer Res* **9**:402–414.

Eklund H, Uhlin U, Färnegårdh M, Logan DT, and Nordlund P (2001) Structure and function of the radical enzyme ribonucleotide reductase. *Prog Biophys Mol Biol* **77**:177–268.

Ellgaard L, and Helenius A (2003) Quality control in the endoplasmic reticulum. *Nat Rev Mol Cell Biol* **4**:181–191.

Enyedy ÉA, Nagy N V., Zsigó É, Kowol CR, Arion VB, Keppler BK, and Kiss T (2010) Comparative Solution Equilibrium Study of the Interactions of Copper(II), Iron(II) and Zinc(II) with Triapine (3-Aminopyridine-2-carbaldehyde Thiosemicarbazone) and Related Ligands. *Eur J Inorg Chem* **2010**:1717–1728.

Enyedy ÉA, Primik MF, Kowol CR, Arion VB, Kiss T, and Keppler BK (2011) Interaction of Triapine and related thiosemicarbazones with iron(III)/(II) and gallium(III): a comparative solution equilibrium study. *Dalton Trans* **40**:5895–5905.

Finch R, Liu M, Cory AH, Cory JG, and Sartorelli AC (1999) Triapine (3-aminopyridine-2-carboxaldehyde thiosemicarbazone; 3-AP): an inhibitor of ribonucleotide reductase with antineoplastic activity. *Adv Enzyme Regul* **39**:3.

Finch RA, Liu M, Grill SP, Rose WC, Loomis R, Vasquez KM, Cheng Y, and Sartorelli AC (2000) Triapine (3-aminopyridine-2-carboxaldehyde- thiosemicarbazone): A potent inhibitor of ribonucleotide reductase activity with broad spectrum antitumor activity. *Biochem Pharmacol* **59**:983–91.

Gomes A, Fernandes E, and Lima JLFC (2005) Fluorescence probes used for detection of reactive oxygen species. *J Biochem Biophys Methods* **65**:45–80.

Gotoh T, Terada K, Oyadomari S, and Mori M (2004) hsp70-DnaJ chaperone pair prevents nitric oxide- and CHOP-induced apoptosis by inhibiting translocation of Bax to mitochondria. *Cell Death Differ* **11**:390–402.

Gupta S, Cuffe L, Szegezdi E, Logue SE, Neary C, Healy S, and Samali A (2010) Mechanisms of ER Stress-Mediated Mitochondrial Membrane Permeabilization. *Int J Cell Biol* **2010**:1–10.

Gupta S, Deepti A, Deegan S, Lisbona F, Hetz C, and Samali A (2010) HSP72 Protects Cells from ER Stress-induced Apoptosis via Enhancement of IRE1α-XBP1 Signaling through a Physical Interaction. *PLoS Biol* **8**:e1000410.

Hancock CN, Stockwin LH, Han B, Divelbiss RD, Jun JH, Malhotra S V, Hollingshead MG, and Newton DL (2011) A copper chelate of thiosemicarbazone NSC 689534 induces oxidative/ER stress and inhibits tumor growth in vitro and in vivo. *Free Radic Biol Med* **50**:110–121.

Harding HP, Zhang Y, Zeng H, Novoa I, Lu PD, Calfon M, Sadri N, Yun C, Popko B, Paules R, Stojdl DF, Bell JC, Hettmann T, Leiden JM, and Ron D (2003) An Integrated Stress Response Regulates Amino Acid Metabolism and Resistance to Oxidative Stress. *Mol Cell* **11**:619–633.

Healy SJM, Gorman AM, Mousavi-Shafaei P, Gupta S, and Samali A (2009) Targeting the endoplasmic reticulum-stress response as an anticancer strategy. *Eur J Pharmacol* **625**:234–246.

Kowol CR, Heffeter P, Miklos W, Gille L, Trondl R, Cappellacci L, Berger W, and Keppler BK (2012) Mechanisms underlying reductant-induced reactive oxygen species formation by anticancer copper(II) compounds. *J Biol Inorg Chem* **17**:409–423.

Kowol CR, Trondl R, Arion VB, Jakupec MA, Lichtscheidl I, and Keppler BK (2010) Fluorescence properties and cellular distribution of the investigational anticancer drug triapine (3-aminopyridine-2-carboxaldehyde thiosemicarbazone) and its zinc(II) complex. *Dalton Trans* **39**:704–706.

Kowol CR, Trondl R, Heffeter P, Arion VB, Jakupec MA, Roller A, Galanski M, Berger W, and Keppler BK (2009) Impact of metal coordination on cytotoxicity of 3-aminopyridine-2-carboxaldehyde thiosemicarbazone (triapine) and novel insights into terminal dimethylation. *J Med Chem* **52**:5032–5043.

Kunos CA, Waggoner S, Gruenigen V Von, Eldermire E, Pink J, Dowlati A, and Kinsella TJ (2010) Phase I Trial of Pelvic Radiation , Weekly Cisplatin , and 3-Aminopyridine-2-Carboxaldehyde Thiosemicarbazone (3-AP , NSC # 663249) for Locally Advanced Cervical Cancer. *Clin Cancer Res* **16**:1298–1306.

Kwon MJ, Oh E, Lee S, Roh MR, Kim SE, Lee Y, Choi Y-L, In Y-H, Park T, Koh SS, and Shin YK (2009) Identification of novel reference genes using multiplatform expression data and their validation for quantitative gene expression analysis. *PLoS ONE* **4**:e6162.

Lee A-H, Iwakoshi NN, and Glimcher LH (2003) XBP-1 regulates a subset of endoplasmic reticulum resident chaperone genes in the unfolded protein response. *Mol Cell Biol* **23**:7448–7459.

Lee AS (2007) GRP78 induction in cancer: therapeutic and prognostic implications. *Cancer Res* **67**:3496–3499.

Lovejoy DB, Jansson PJ, Brunk UT, Wong J, Ponka P, and Richardson DR (2011) Antitumor activity of metal-chelating compound Dp44mT is mediated by formation of a redox-active copper complex that accumulates in lysosomes. *Cancer Res* **71**:5871–5880.

Luo S, and Lee AS (2002) Requirement of the p38 mitogen-activated protein kinase signalling pathway for the induction of the 78 kDa glucose-regulated protein/immunoglobulin heavy-chain binding protein by azetidine stress: activating transcription factor 6 as a target for stress-induced phosphorylation. *Biochem J* **366**:787–795.

Matsumoto M, Minami M, Takeda K, Sakao Y, and Akira S (1996) Ectopic expression of CHOP (GADD153) induces apoptosis in M1 myeloblastic leukemia cells. *FEBS Lett* **395**:143–147.

Maytin E V, Ubeda M, Lin JC, and Habener JF (2001) Stress-inducible transcription factor CHOP/gadd153 induces apoptosis in mammalian cells via p38 kinase-dependent and -independent mechanisms. *Exp Cell Res* **267**:193–204.

McCullough KD, Martindale JL, Klotz LO, Aw TY, and Holbrook NJ (2001) Gadd153 sensitizes cells to endoplasmic reticulum stress by down-regulating Bcl2 and perturbing the cellular redox state. *Mol Cell Biol* **21**:1249–1259.

Nutting CM, van Herpen CML, Miah AB, Bhide SA, Machiels J-P, Buter J, Kelly C, de Raucourt D, and Harrington KJ (2009) Phase II study of 3-AP Triapine in patients with recurrent or metastatic head and neck squamous cell carcinoma. *Ann Oncol* **20**:1275–1279.

Ocean AJ, Christos P, Sparano J a, Matulich D, Kaubish A, Siegel A, Sung M, Ward MM, Hamel N, Espinoza-Delgado I, Yen Y, and Lane ME (2011) Phase II trial of the ribonucleotide reductase inhibitor 3-aminopyridine-2-carboxaldehydethiosemicarbazone plus gemcitabine in patients with advanced biliary tract cancer. *Cancer Chemother Pharmacol* **68**:379–388.

Oyadomari S, and Mori M (2004) Roles of CHOP/GADD153 in endoplasmic reticulum stress. *Cell Death Differ* **11**:381–389.

Pfaffl MW, Horgan GW, and Dempfle L (2002) Relative expression software tool (REST) for group-wise comparison and statistical analysis of relative expression results in real-time PCR. *Nucleic Acids Res* **30**:e36.

Puthalakath H, O'Reilly LA, Gunn P, Lee L, Kelly PN, Huntington ND, Hughes PD, Michalak EM, McKimm-Breschkin J, Motoyama N, Gotoh T, Akira S, Bouillet P, and Strasser A (2007) ER stress triggers apoptosis by activating BH3-only protein Bim. *Cell* **129**:1337–1349.

Pyrko P, Schönthal AH, Hofman FM, Chen TC, and Lee AS (2007) The unfolded protein response regulator GRP78/BiP as a novel target for increasing chemosensitivity in malignant gliomas. *Cancer Res* **67**:9809–9816.

Ron D, and Walter P (2007) Signal integration in the endoplasmic reticulum unfolded protein response. *Nat Rev Mol Cell Biol* **8**:519–529.

Salvioli S, Ardizzoni A, Franceschi C, and Cossarizza A (1997) JC-1, but not DiOC6(3) or rhodamine 123, is a reliable fluorescent probe to assess $\Delta\Psi$ changes in intact cells: implications for studies on mitochondrial functionality during apoptosis. *FEBS Lett* **411**:77–82.

Schmitt E, Naveau M, and Mechulam Y (2010) Eukaryotic and archaeal translation initiation factor 2: a heterotrimeric tRNA carrier. *FEBS Lett* **584**:405–412.

Shao J, Zhou B, Di Bilio AJ, Zhu L, Wang T, Qi C, Shih J, and Yen Y (2006) A Ferrous-Triapine complex mediates formation of reactive oxygen species that inactivate human ribonucleotide reductase. *Mol Cancer Ther* **5**:586–592.

Suzuki T, Lu J, Zahed M, Kita K, and Suzuki N (2007) Reduction of GRP78 expression with siRNA activates unfolded protein response leading to apoptosis in HeLa cells. *Arch Biochem Biophys* **468**:1–14.

Szegezdi E, Logue SE, Gorman AM, and Samali A (2006) Mediators of endoplasmic reticulum stress-induced apoptosis. *EMBO Rep* **7**:880–885.

Traynor AM, Lee J-W, Bayer GK, Tate JM, Thomas SP, Mazurczak M, Graham DL, Kolesar JM, and Schiller JH (2010) A phase II trial of triapine (NSC# 663249) and gemcitabine as second line treatment of advanced non-small cell lung cancer: Eastern Cooperative Oncology Group Study 1503. *Invest New Drugs* **28**:91–97.

Urano F, Wang X, Bertolotti A, Zhang Y, Chung P, Harding HP, and Ron D (2000) Coupling of stress in the ER to activation of JNK protein kinases by transmembrane protein kinase IRE1. *Science* **287**:664–666.

Weston CR, and Davis RJ (2007) The JNK signal transduction pathway. *Curr Opin Cell Biol* **19**:142–149.

Wijerathna SR, Ahmad MF, Xu H, Fairman JW, Zhang A, Kaushal PS, Wan Q, Kiser J, and Dealwis CG (2011) Targeting the Large Subunit of Human Ribonucleotide Reductase for Cancer Chemotherapy. *Pharmaceuticals* **4**:1328–1354.

Xu C, Bailly-Maitre B, and Reed JC (2005) Endoplasmic reticulum stress: cell life and death decisions. *J Clin Invest* **115**:2656–2664, Am Soc Clin Investig.

Yamaguchi H, and Wang H-G (2004) CHOP is involved in endoplasmic reticulum stress-induced apoptosis by enhancing DR5 expression in human carcinoma cells. *J Biol Chem* **279**:45495–45502.

Yen Y, Grill SP, Dutschman GE, Chang CN, Zhou BS, and Cheng YC (1994) Characterization of a hydroxyurea-resistant human KB cell line with supersensitivity to 6-thioguanine. *Cancer Res* **54**:3686–3691.

Yoshida H, Matsui T, Yamamoto A, Okada T, and Mori K (2001) XBP1 mRNA is induced by ATF6 and spliced by IRE1 in response to ER stress to produce a highly active transcription factor. *Cell* **107**:881–891.

Yu Y, and Richardson DR (2011) Cellular iron-depletion stimulates the JNK and p38 MAP signaling transduction pathways, dissociation of ASK1-thioredoxin and activation of ASK1. *J Biol Chem* **286**:15413–15427.

Zuker M (2003) Mfold web server for nucleic acid folding and hybridization prediction. *Nucleic Acids Res* **31**:3406–3415.

Footnotes. This work was supported by the Johanna Mahlke née Obermann Foundation for Cancer Research and the Austrian Science Fund (FWF) [Grant P22072-B11]

Part of this work was previously presented at the following conference: Trondl R, Jungwirth U, Heffeter P, Kowol CR, Arion VB, Jakupec MA, Keppler BK (2011) Terminal dimethyl substitution of Triapine leads to activation of CHOP and induction of apoptosis via ER stress in human colon cancer cells. In: *Proceedings of the 102nd Annual Meeting of the American Association for Cancer Research (AACR)*, Orlando, Florida

Michael Jakupec PhD, Institute of Inorganic Chemistry, University of Vienna, Waehringer Strasse 42, Vienna 1090, Austria E-mail: michael.jakupec@univie.ac.at

Figure Legends

Figure 1. Chemical structures and absorption/emission spectra of 3-AP and 3-AP-Me. A) Structural formula of 3-AP and 3-AP-Me. B) UV/vis absorption spectrum of 3-AP (black solid line) and 3-AP-Me (grey solid line) (c_L = 0.05 mM) and fluorescence emission spectrum of 3-AP (black dashed line) and 3-AP-Me (gray dashed line) (c_L = 0.01 mM; λ_{EX} = 360 nm), pH 7.4 in 30% (w/w) DMSO/H_2O, t = 25.0 °C, I = 0.10 M (KCl).

Figure 2. Live cell fluorescence microscopy images of SW480 colon carcinoma cells. Cells were co-stained in a stepwise procedure in a flow cell with 100 µM (A) 3-AP or (B) 3-AP-Me and ER-Tracker Green (1 µM) or Mito-Tracker Red (200 nM) for 5 min each. After each staining step, cells were washed three times with PBS. Insert depicts higher magnification. Scale bar is 20 µm.

Figure 3. 3-AP and 3-AP-Me induces key factors of the unfolded protein response. (A) Western blot analysis of PERK, eIF2α phosphorylation, calreticulin, calnexin, CHOP and GRP78 were analyzed in SW480 and HCT-116 colon carcinoma cells after 3-AP or 3-AP-Me treatment. 0.5 µM Thapsigargin (Tha) was used a positive control. Shown results are representatives out of three independent experiments. (B) Change in gene expression of CHOP and GRP78 mRNA measured by RT-qPCR in SW480 and HCT-116 cells were treated for 24 h at the indicated concentrations. (C) Change in gene expression of splicing variants of XBP1 mRNA and activation of the transcription factors ATF4 and ATF6 measured by RT-qPCR. SW480 or HCT-116 cells were treated with indicated concentration of 3-AP or 3-AP-Me for 24 h. Bars display means ± S.D. of three independent experiments (n=6); *$p < 0.05$;**$p < 0.01$; ***$p < 0.001$, compared with control, as calculated by a one-way ANOVA test.

Figure 4. 3-AP and 3-AP-Me activate the cellular stress kinases p38 MAPK and JNK and trigger Bim expression. (A) Western blot analysis of JNK and p38 MAPK phosphorylation in SW480 and HCT-116 cells after 12 h treatment. Expression of the three Bim isoforms (Bim_{EL}, Bim_L and Bim_S) was analyzed by

Western blot after 24 h. Cells were treated with 1, 5, 25 or 50 µM of 3-AP or 3-AP-Me. Results shown are representatives out of three independent experiments. (B) Cytotoxic effects of 3-AP or 3-AP-Me were analyzed with co-incubation of 1.25 µM cycloheximide (CHX) and 10 µM JNK inhibitor SP600125 in HCT-116 cells after 72 h by the MTT assay. IC_{50} values and % survival are displayed for 6 independent experiments (n=6). Columns display means ± S.D. *$p < 0.05$;**$p < 0.01$; ***$p < 0.001$, compared with 3-AP or 3-AP-Me alone, as calculated by a one-way ANOVA test.

Figure 5. Depolarization of mitochondrial membranes by 3-AP and 3-AP-Me, detected by flow cytometric analysis upon JC-1 staining. JC-1 forms aggregates (orange fluorescence) under normal membrane potential, while in depolarized mitochondrial membranes JC-1 dissociates to monomers (green fluorescence). HL-60 leukemia cells were treated with 0.25, 0.5 or 1 µM 3-AP or 3-AP-Me for 24 h. Results shown are representatives out of three independent experiments.

Figure 1

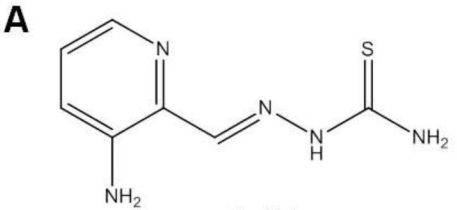

3-AP

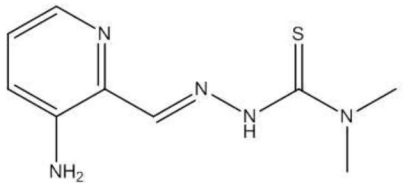

3-AP-Me

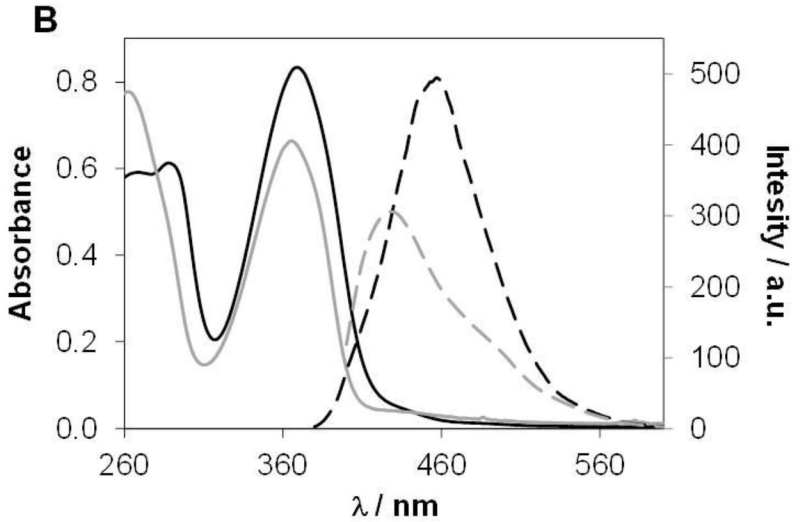

Figure 2

A

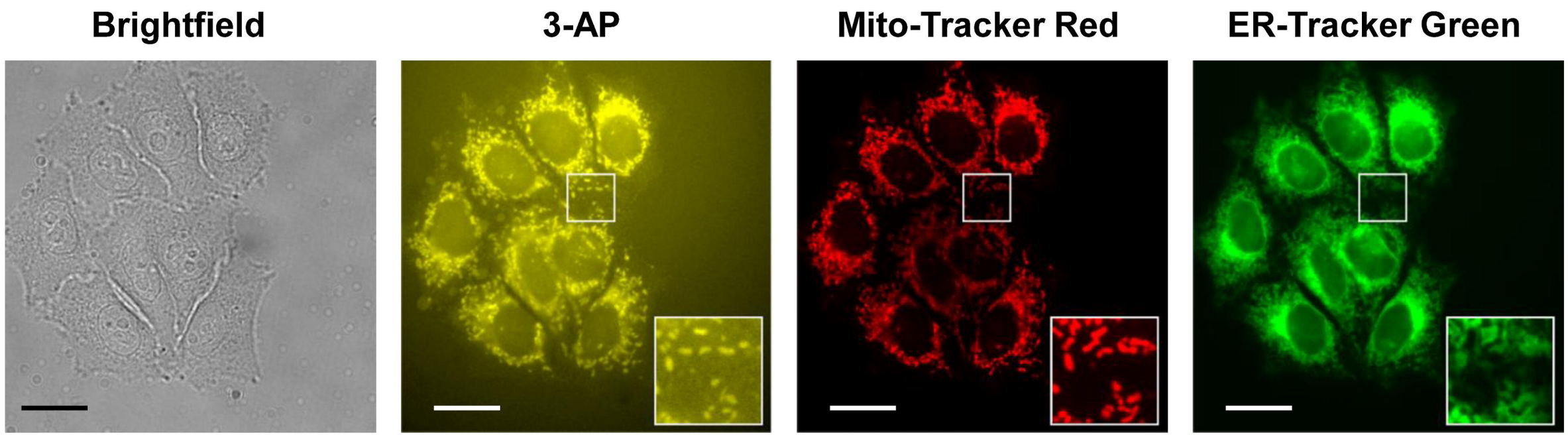
Brightfield
3-AP
Mito-Tracker Red
ER-Tracker Green

B

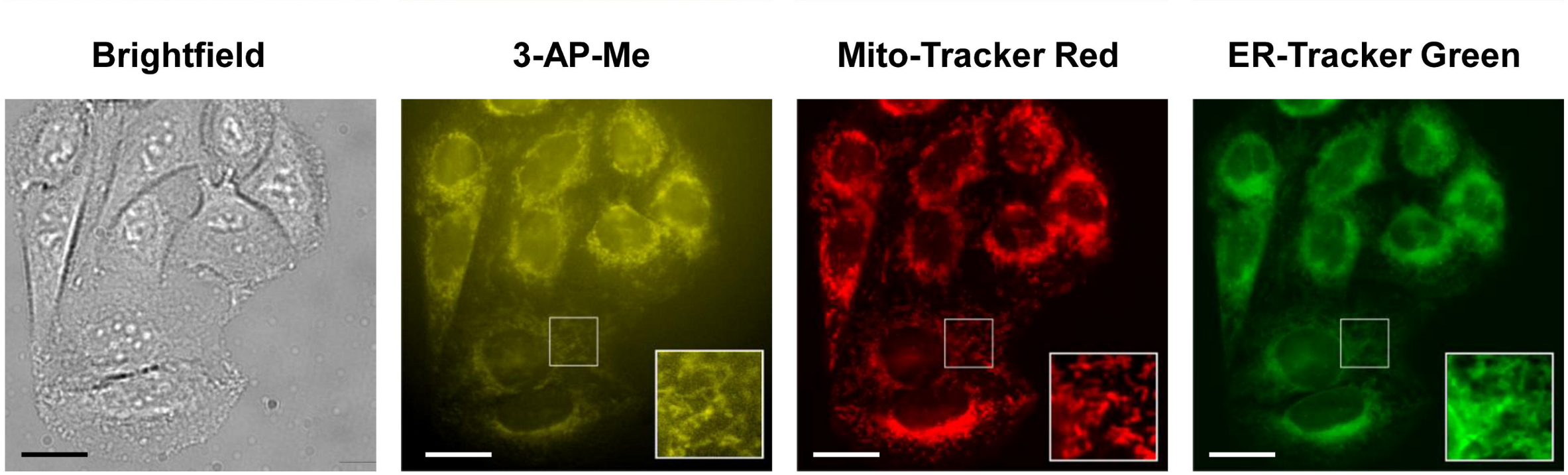
Brightfield
3-AP-Me
Mito-Tracker Red
ER-Tracker Green

Figure 3

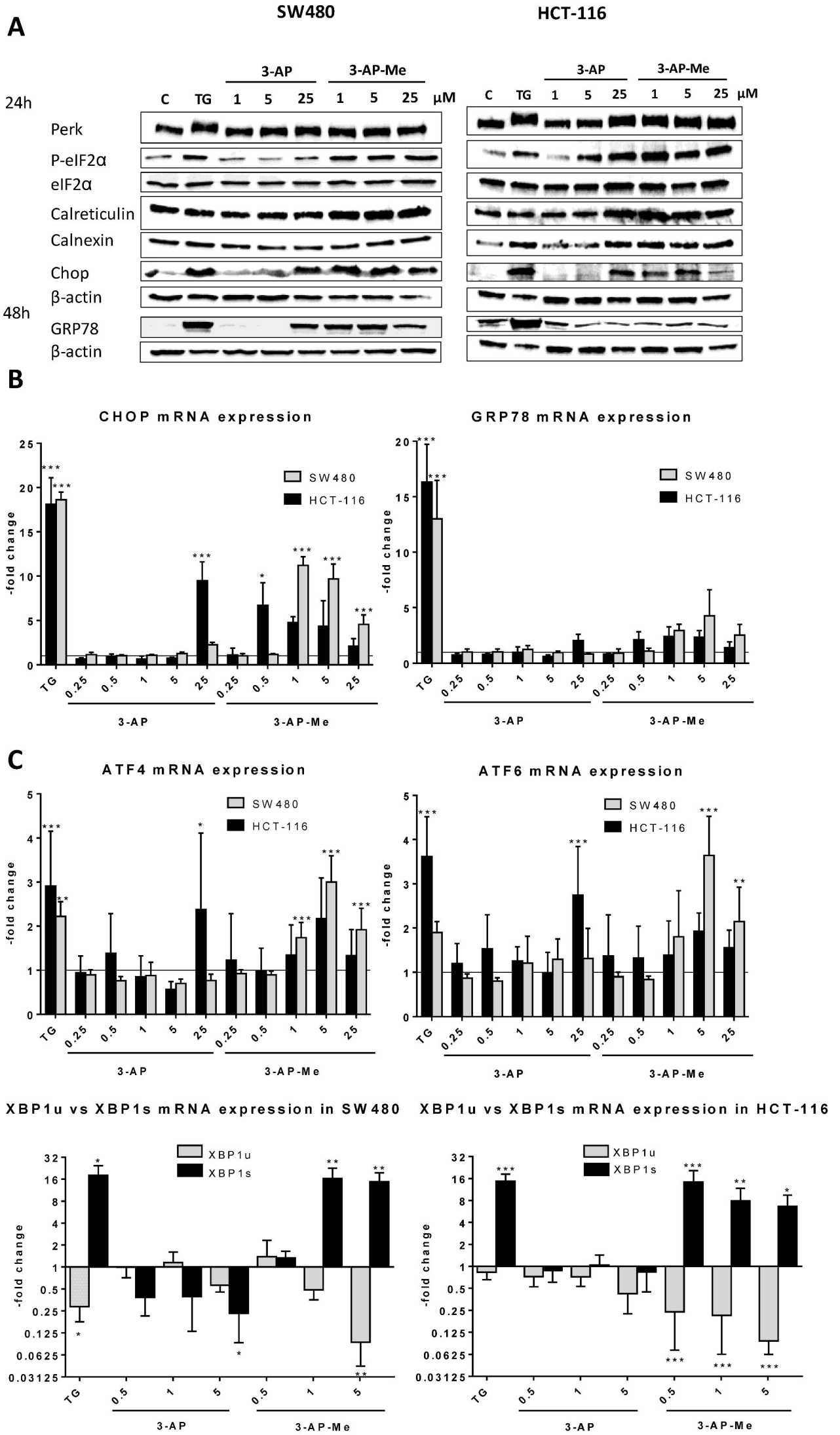
A
SW480
HCT-116
3-AP
3-AP-Me
C
TG
1
5
25
1
5
25
μM
24h
Perk
P-eIF2α
eIF2α
Calreticulin
Calnexin
Chop
β-actin
48h
GRP78
β-actin
B
CHOP mRNA expression
GRP78 mRNA expression
SW480
HCT-116
-fold change
TG
0.25
0.5
1
5
25
3-AP
3-AP-Me
C
ATF4 mRNA expression
ATF6 mRNA expression
XBP1u vs XBP1s mRNA expression in SW480
XBP1u vs XBP1s mRNA expression in HCT-116
XBP1u
XBP1s

Figure 4

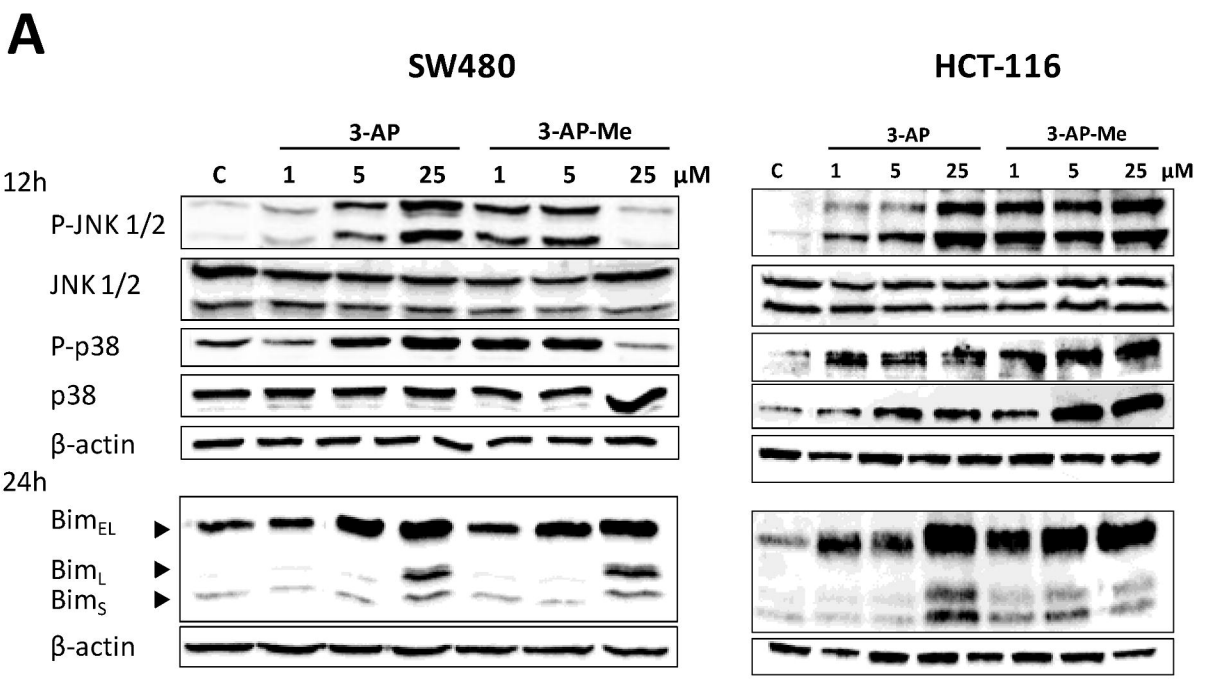

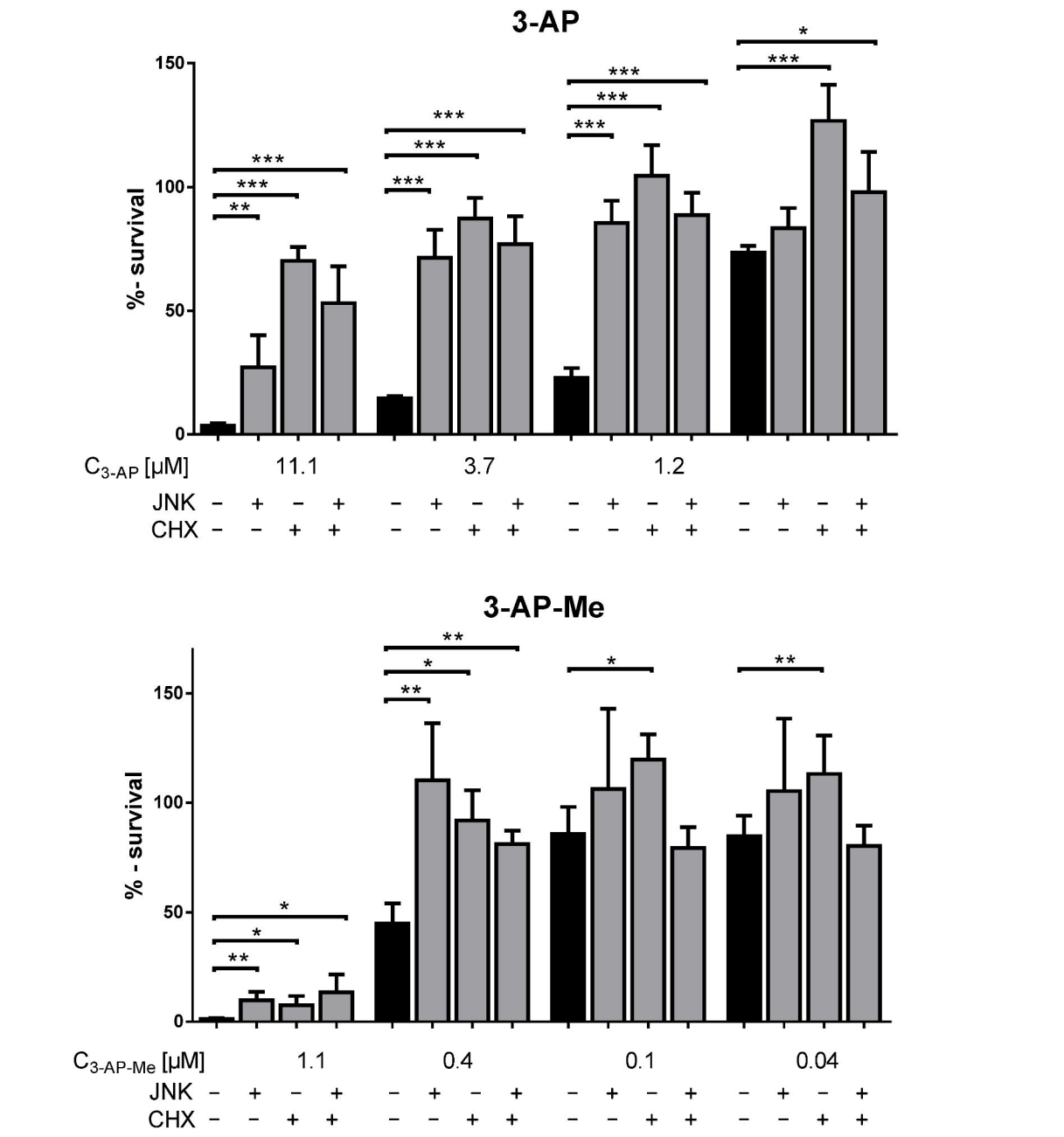

		3-AP		
CHX	-	+	-	+
JNK Inhibitor	-	-	+	+
IC_{50} [µM]	0.76	6.52 ***	15.8 ***	12.3 ***
		3-AP-Me		
CHX	-	+	-	+
JNK Inhibitor	-	-	+	+
IC_{50} [µM]	0.33	0.70 ***	0.68 ***	0.67 **

Figure 5

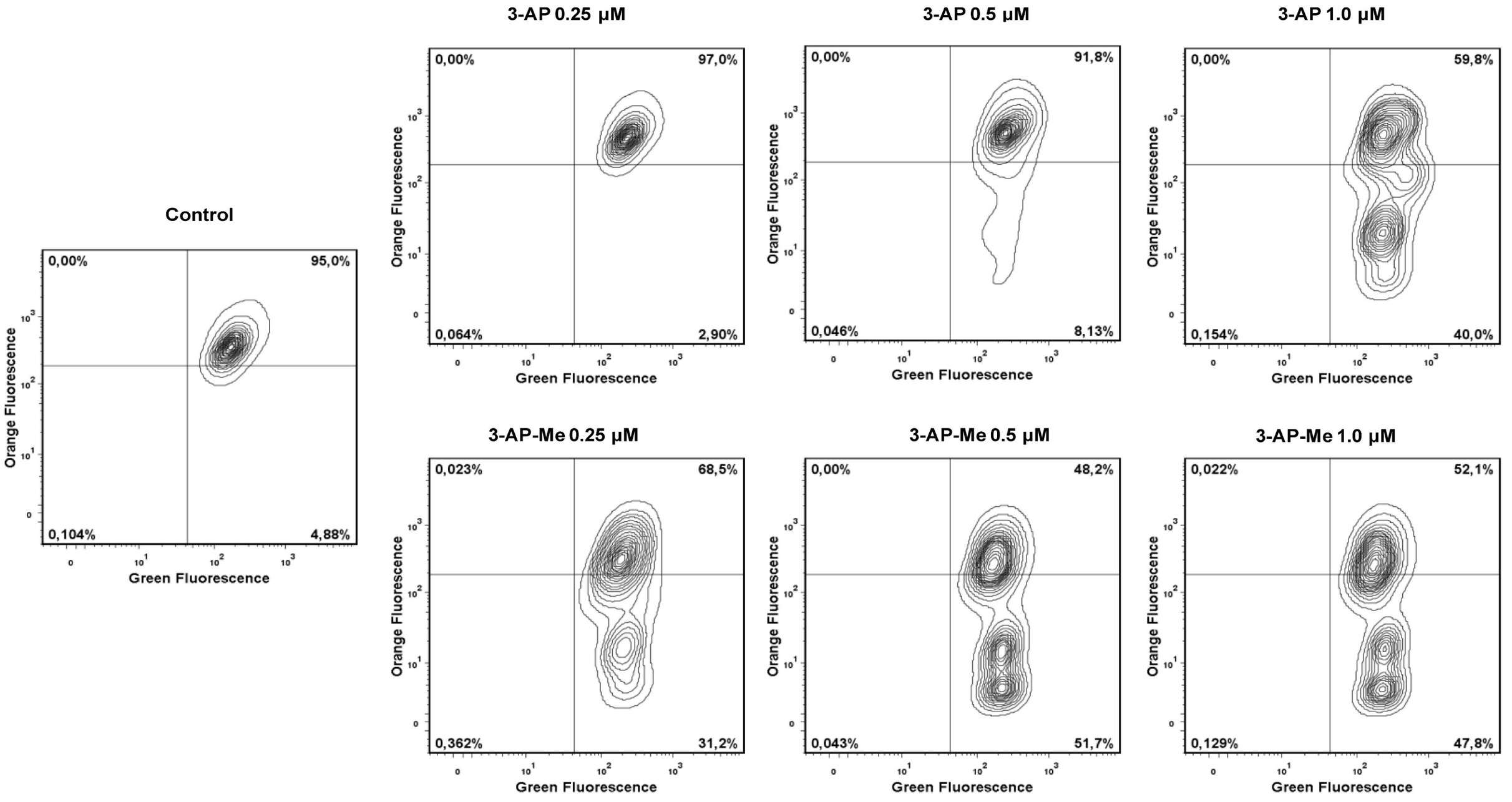
Control
0,00%
95,0%
0,104%
4,88%
3-AP 0.25 µM
0,00%
97,0%
0,064%
2,90%
3-AP 0.5 µM
0,00%
91,8%
0,046%
8,13%
3-AP 1.0 µM
0,00%
59,8%
0,154%
40,0%
3-AP-Me 0.25 µM
0,023%
68,5%
0,362%
31,2%
3-AP-Me 0.5 µM
0,00%
48,2%
0,043%
51,7%
3-AP-Me 1.0 µM
0,022%
52,1%
0,129%
47,8%
Orange Fluorescence
Green Fluorescence